Role of Local Dynamics in the Gas Permeability of Glassy Substituted Polyacetylenes. A Quasielastic Neutron Scattering Study

Toshiji Kanaya,*,† Itaru Tsukushi,‡ Keisuke Kaji,† Toshikazu Sakaguchi,§ Giseop Kwak,§ and Toshio Masuda§

Institute for Chemical Research, Kyoto University, Uji, Kyoto-fu 611-0011, Japan; Chiba Institute of Technology, Narashino, Chiba-ken, 275-0023, Japan; and Department of Polymer Chemistry, Kyoto University, Kyoto 606-8501, Japan

Received March 7, 2002

ABSTRACT: The local dynamics of 10 substituted polyacetylenes in the glassy state have been investigated using a quasielastic neutron scattering technique in a time range of picoseconds to several tens of picoseconds to see a relationship between the local mobility and the gas permeability of these polymers. Even in the glassy state, these polymers show quasielastic scattering components, suggesting that certain stochastic motions occur in the glassy state. The dynamic scattering laws $S(Q,\omega)$ of the quasielastic components were well fitted to the sum of two Lorentzians, i.e., the narrow (slow) and broad (fast) components. It was found that both the relaxation rate Γ_n and the fraction A_n of the narrow (slow) component show positive correlations with oxygen permeability coefficient (P_{O_2}), suggesting that the local mobility of the matrix polymers plays an important role in gas permeability. We then defined local flux F, which is the product of Γ_n and A_n, as a measure of the local mobility to find that F is proportional to the diffusion coefficient of O_2 gas (D_{O_2}), i.e., $F \propto D_{O_2}$. To explain and discuss this relation, we have proposed a random gate model, where mobile side groups in the matrix polymer act as a gate for gas diffusion.

Introduction

It is now well-known that many polyacetylenes with bulky substituents exhibit high gas permeability among all the existing polymers.[1−3] Among them, poly[1-(trimethylsilyl)-1-propyne] [poly(TMSP)] shows extremely high permeability to various gases, e.g., the oxygen permeability coefficient (P_{O_2}) ∼ 4000 barrers [1 barrer = 1×10^{-10} cm^3 (STP) cm/(cm^2 s cmHg) (25 °C)].[3−8] The high gas permeability of poly(TMSP) has been attributed to the presence of microvoids due to poor polymer chain packing, which is confirmed by low density and high free volume.[3] This polymer is glassy at room temperature unlike poly(dimethylsiloxane) [poly(DMS)], which is also known as highly gas permeable polymer. The gas permeation through poly(TMSP) is explained in terms of the dual-mode sorption and diffusion mechanism, which involves both the Langmuir-type adsorption and the Henry-type solution. If a methyl on the silyl group in this polymer is replaced by bulkier substituents, the polymers generally show a lower gas permeability.[9,10]

Another type of Si-containing disubstituted acetylene polymer, poly[1-phenyl-2-(*p*-trimethylsilylphenyl)acetylene] [poly(*p*-Me_3SiDPA)], also permeates gases fairly well.[11−13] Thus, its P_{O_2} value is 1100 barrers (25 °C), corresponding to about $^1/_4$ that of poly(TMSP) and about twice that of poly(DMS). The high gas permeability of this polymer is explained similarly to the case of poly(TMSP).[13] It is interesting that poly[1-phenyl-2-(*p*-*tert*-butylphenyl)acetylene] [poly(*p*-*t*-BuDPA)][14] and poly[1-phenyl-2-(*m*-trimethylgermylphenyl)acetylene] [poly(*m*-Me_3GeDPA)][15] permeate gases as well as poly(*p*-Me_3SiDPA). The high gas permeability of poly(TMSP) and these poly(diphenylacetylene) derivatives suggests that both stiff main chain and spherical side groups play an important role in the gas permeation through substituted polyacetylene membranes.

Regarding substituent effects, it has turned out that the P_{O_2} values (25 °C) of poly[1-phenyl-2-(*p*-triisopropylsilylphenyl)acetylene] [poly(*p*-*i*Pr_3SiDPA)] and poly[1-phenyl-2-(*p*-triphenylsilylphenyl)acetylene] [poly(*p*-Ph_3SiDPA)] are 20 and 3.8 barrers, respectively,[16,17] which are much smaller than that of poly(*p*-Me_3SiDPA). This fact along with the finding about the substituent effect in poly(TMSP)[9,10] (see above) suggests that bulky spherical substituents are not necessarily favorable for high gas permeability, which was apparently difficult for us to understand. Our speculation for the relatively low permeability of poly(*p*-*i*Pr_3SiDPA) and poly(*p*-Ph_3SiDPA) is that, if the spherical substituent is too large, its mobility in the glassy state is extremely low, which leads to low permeability. To confirm this speculation, we need information on the local dynamics of these polymers in the glassy state.

A quasielastic neutron scattering (QENS) technique is one of the most powerful methods for investigation of molecular motions in a time range of 10^{-13}−10^{-8} s.[18] In the measurements, the scattering intensity is recorded as functions of energy and momentum transfer of neutrons, providing information about both time and spatial scales of the motions simultaneously. Thus, this QENS technique has been extensively applied for studies on the dynamics of polymers in the glassy state[19,20] as well as near the glass transition temperature.[21−23]

In preliminary studies,[24,25] we have investigated the local mobility of three substituted polyacetylenes in the glassy state by means of the QENS technique to find that the local mobility is an important factor controlling gas permeability. In this work, we have extended our QENS study to 10 substituted polyacetylenes in the glassy state to confirm the previous finding and gain

† Institute for Chemical Research, Kyoto University.
‡ Chiba Institute of Technology.
§ Department of Polymer Chemistry, Kyoto University.
* Corresponding author: Tel +81-774-38-3141; Fax +81-774-38-3146; e-mail kanaya@scl.kyoto-u.ac.jp.

10.1021/ma0203546 CCC: $22.00
Published on Web 06/06/2002

Table 1. Chemical Structure of Side Groups (X_1 and X_2) of Substituted Polyacetylenes, Permeability Coefficient P_{O_2}, Diffusion Coefficient D_{O_2}, Solubility Coefficient S_{O_2} and Root-Mean-Square Displacement $\langle l^2 \rangle^{1/2}$ for the Jump Motion of Oxygen Gas

		$(-CX_1=CX_2-)_n$					
code	polymer	X_1	X_2	$P_{O_2} \times 10^8$ [a]	$D_{O_2} \times 10^6$ [b]	$S_{O_2} \times 10^2$ [c]	$\langle l^2 \rangle^{1/2}$ (Å)
1	poly(TMSP)	Me	$SiMe_3$	40−100 [d]	18.0	2.22	3.2
2	poly(*p*-Me_3SiDPA)	Ph	C_6H_4-*p*-$SiMe_3$	11.0 [e]	7.70	1.43	2.2
3	poly(*p*-*i*PrSiDPS)	Ph	C_6H_4-*p*-Si(*i*-Pr)$_3$	0.20 [f]	0.92	0.22	5.2
4	poly(*p*-AdDPA)	Ph	C_6H_4-*p*-adamanyl	0.55 [g]	0.80	0.69	1.9
5	poly(*p*-*t*BuDPA)	Ph	C_6H_4-*p*-*t*-Bu	11.0 [h]	6.90	1.59	4.7
6	poly(*p*-*n*BuDPA)	Ph	C_6H_4-*p*-*n*-Bu	1.0 [h]	2.10	0.48	2.8
7	poly(*p*-Ph_3SiDPA)	Ph	C_6H_4-*p*-$SiPh_3$	0.038 [g]	0.32	0.12	5.6
8	poly(*p*-PhODPA)	Ph	C_6H_4-*p*-OPh	0.37 [i]	0.58	0.64	8.1
9	poly(TBA)	H	*t*-Bu	1.2 [j]	2.92	0.41	3.7
10	poly(*p*-Et_3SiDPA)	Ph	C_6H_4-*p*-$SiEt_3$	0.95	3.10	0.31	4.9

[a] In cm^3 (STP) cm cm^{-2} s^{-1} $cmHg^{-1}$. [b] In cm^2 s^{-1}. [c] In cm^3 (STP) cm^{-3} $cmHg^{-1}$. [d] Reference 3. [e] Reference 11. [f] Reference 16. [g] Reference 38. [h] Reference 14. [i] Reference 39. [j] Reference 26.

knowledge about gas permeation mechanism through glassy polymers. The relationship between the local mobility and the gas permeability is discussed.

Experimental Section

Materials. Substituted polyacetylenes used in this experiment are listed in Table 1 with their chemical structures.

Polymerizations for the synthesis of the polymers were carried out under dry nitrogen according to the procedure described before.[4,12,26] The polymerization conditions are as follows: for poly(TMSP) (Table 1, code 1): in toluene, 80 °C, 24 h, $[M]_0$ = 1.0 mol/L, $[TaCl_5]$ = 20 mmol/L; for the poly(diphenylacetylene) derivatives (Table 1, codes 2−8, 10): in toluene, 80 °C, 24 h, $[M]_0$ = 0.50 mol/L, $[TaCl_5]$ = 20 mmol/L, $[n\text{-}Bu_4Sn]$ = 40 mmol/L; for poly(TBA) (Table 1, code 9): in toluene, 30 °C, 24 h, $[M]_0$ = 1.0 mol/L, $[MoCl_5]$ = 20 mmol/L. Polymerizations were quenched with a toluene/methanol (volume ratio, 4:1) mixture. The polymerization mixtures were diluted with toluene and poured into a large amount of methanol under stirring to precipitate the formed polymers. The precipitated polymers were filtered off and dried under vacuum at room temperature. The free-standing films (thickness >150 μm) of these polymers were obtained by a solution casting method using toluene as solvent.

They are in the glassy state at room temperature. The glass transition temperatures T_g are much higher than room temperature although the exact values are not measurable due to the chemical decomposition.

Gas Permeability Measurements. The oxygen permeation was observed on a Rikaseiki K-315-N gas permeability apparatus. The oxygen permeability coefficients (P_{O_2}) were determined by using the following equation.

$$P = \frac{qhd}{tap} \tag{1}$$

Here, q, h, and d are the amounts of permeate (cm^3), calibration coefficient, and membrane thickness (cm), respectively, and t, a, and p are permeation time (s), membrane area (cm^2), and partial pressure (cmHg), respectively.

Diffusion coefficients (D_{O_2}) were measured by the time-lag method using the following equation:

$$D = \frac{d^2}{6\theta} \tag{2}$$

where θ is time lag. Solubility coefficients (S_{O_2}) were calculated using $S = P/D$. The obtained permeability coefficient P_{O_2}, diffusion coefficient D_{O_2}, and solubility coefficient S_{O_2} are listed in Table 1.

Quasielastic Neutron Scattering Measurements. Quasielastic neutron scattering (QENS) measurements were performed on the time-of-flight (TOF) spectrometer AGNES[27] installed at the C3-1 cold neutron guide in JRR-3M reactor, Tokai. The incident wavelength of neutrons was 4.22 Å, giving an energy resolution $\Delta\epsilon$ of 0.08 meV evaluated from the full width at half-maximum (fwhm) at the elastic position. Energy transfer $\Delta E = \hbar\omega$ ranges from −2 to 20 meV, where ΔE is defined as negative for energy loss of neutrons. 160 detectors at scattering angles from 8° to 120° were grouped into 10 groups, covering a Q (length of scattering vector) range of 0.2−2.6 $Å^{-1}$. The amount of sample was chosen so that the total scattering intensity would be about 10% of the incident neutrons to reduce multiple scattering. The observed TOF spectra were converted to symmetrized dynamic scattering laws $S(Q,\omega)$ after correcting empty can scattering and counter efficiency.

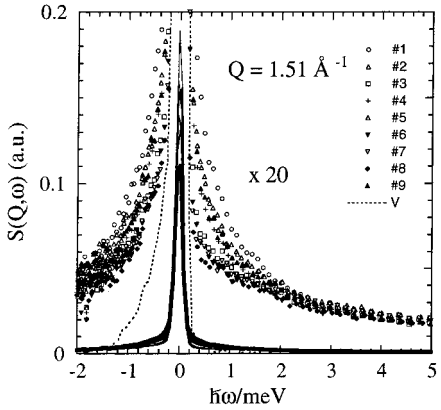

Figure 1. Dynamic scattering laws $S(Q,\omega)$ of substituted polyacetylenes (1−9) which have been normalized to the total scattering intensity in an energy range between 0 and 20 meV. Average Q value is 1.51 $Å^{-1}$. Dashed line is a resolution function determined by a vanadium measurement. For the sample codes, see Table 1.

Results and Discussion

Observed dynamic scattering laws $S(Q,\omega)$ for nine substituted polyacetylenes are shown in Figure 1, where the spectra expanded by a factor of 20 are also displayed to see the detail. These spectra were obtained by summing up all spectra at various Q's ranging from 0.36 to 2.5 $Å^{-1}$ to get higher counting statistics and normalized to the total scattering intensity in the energy region between 0 and 20 meV. The average Q value of the spectra is 1.51 $Å^{-1}$. A very strong peak at around $\hbar\omega$ = 0 is due to elastic scattering within the energy resolution of the spectrometer. This strong elastic scattering suggests that molecular motions are almost frozen in these polymers. This is very natural because these polymers are in the glassy states. However, looking at the expanded spectra, small but clear quasielastic scattering is observed on the wings of the elastic

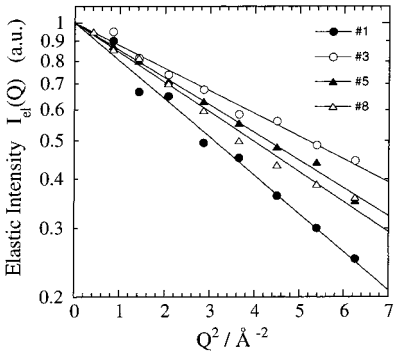

Figure 2. Q dependence of elastic scattering intensity $I_{el}(Q)$. The lines are the results of fit using $I_{el}(Q) = \exp[-1/3\langle u^2\rangle Q^2]$: (●) sample 1, (○) sample 3, (▲) sample 5, (△): sample 8.

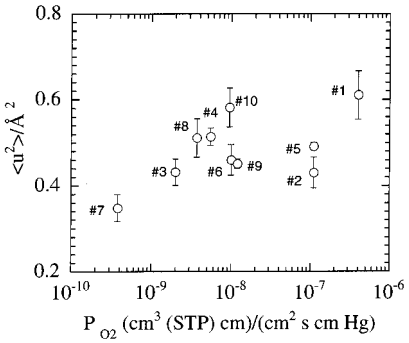

Figure 3. Mean-square displacements $\langle u^2\rangle$ evaluated from the fits in Figure 2 as a function of permeability coefficient P_{O_2}.

scattering, suggesting that molecules are performing stochastic motions even in the glassy state.

First we focus our attention on the Q dependence of the elastic scattering intensity $I_{el}(Q)$. The scattering intensity from the substituted polyacetylenes is mainly governed by incoherent scattering of hydrogen atoms because incoherent scattering cross section of hydrogen atom is much larger than coherent and incoherent scattering cross sections of other atoms as well as coherent one of hydrogen atom.[28] In the Gaussian approximation, the Q dependence of incoherent elastic scattering intensity is given by

$$I_{el}(Q) = \exp\left[-\frac{1}{3}\langle u^2\rangle Q^2\right] \tag{3}$$

where $\langle u^2\rangle$ is a mean-square displacement, which is a measure of average amplitude of motions of hydrogen atoms outside the energy resolution. The Q dependences of $I_{el}(Q)$ for four substituted polyacetylenes are shown in Figure 2 in a form of log $[I_{el}(Q)]$ vs Q^2, where $I_{el}(Q)$ was normalized to $I_{el}(Q{=}0)$. The solid lines are the results of fit using eq 3. We evaluated $\langle u^2\rangle$ from the slope of the straight lines in Figure 2, which are plotted as a function of P_{O_2} in Figure 3. It seems that a positive correlation exists between $\langle u^2\rangle$ and P_{O_2}, although the data points are somewhat scattered. This suggests that the local motions play some roles in the gas permeability of substituted polyacetylenes. To see the motions of hydrogen atoms directly, we have to analyze the quasielastic scattering.

As seen in Figure 1, the dynamic scattering laws $S(Q,\omega)$ obviously show quasielastic scattering components. In a previous paper,[24] we described this quasielastic component using a single Lorentzian in the energy range from −0.5 to 2.5 meV. However, as shown in the latest paper,[25] the quasielastic scattering component in the wide energy range of −2 to 10 meV cannot be described by a single Lorentzian, but by double Lorentzians. In the present analysis, we therefore employed the following phenomenological function to describe the observed dynamic scattering law $S(Q,\omega)$

$$S(Q,\omega) = [1 - A_n(Q) - A_b(Q)]\delta(\omega) + A_n(Q)L(\Gamma_n,Q,\omega) + A_b(Q)L(\Gamma_b,Q,\omega) + B_{in}(Q) \tag{4}$$

$$L(\Gamma_i,Q,\omega) = \frac{1}{\pi}\frac{\Gamma_i}{\Gamma_i^2 + \omega^2} \quad (i = \text{n and b}) \tag{5}$$

Here, in the right-hand side of eq 4, the first term $[1 - A_n(Q) - A_b(Q)]\delta(\omega)$ represents immobile parts of molecules within the energy resolution, and the second and third terms $A_n(Q)L(\Gamma_n,Q,\omega)$ and $A_b(Q)L(\Gamma_b,Q,\omega)$ describe narrow (slow) and broad (fast) relaxational parts, respectively. The half-widths at half-maximum (hwhm) Γ_i (i = n and b) are the relaxation rates of the narrow (slow) and broad (fast) components, respectively, corresponding to the inverses of the relaxation times, $\tau_i = (1/\Gamma_i)$ (i = n and b). The fourth term $B_{in}(Q)$ represents an inelastic flat background.

The model dynamic scattering law (eq 4) was fitted to the observed spectra after convolution with the resolution function of the spectrometer. The result of the fit is shown in parts a and b of Figure 4 for samples 1 and 5, respectively. The deviation plots of the fits do not show any systematic error, suggesting that the model function (eq 4) is appropriate to describe $S(Q,\omega)$ of these polymers. Then, we evaluated the relaxation rates Γ_n and Γ_b and the fractions A_n and A_b for the narrow and broad components, respectively.

In Figure 5, the relaxation rates Γ_n and Γ_b, corresponding to the inverses of the relaxation times $1/\tau_n$ and $1/\tau_b$, for the narrow and broad components are plotted as a function of oxygen permeability coefficient, P_{O_2}. It is very interesting that the relaxation rate of the narrow component Γ_n clearly shows a correlation with P_{O_2} while Γ_b of the broad component is almost independent of P_{O_2}. This implies that the motion concerning the slow component may play an important role in the gas permeability.

In Figure 6, the fractions of the narrow and broad components A_n and A_b are also plotted against P_{O_2}. A_b is practically constant for all samples, whereas A_n tends to increase with the gas permeability coefficient P_{O_2}, although there are some exceptions such as samples 3, 4, and 9. The change of gas permeability coefficient is less dominated by A_n than the relaxation rate Γ_n because A_n does vary in a range less than 1 order, but the change of Γ_n is more than 2 orders. However, the correlation observed between A_n and P_{O_2} may suggest the fraction A_n also plays some role in the gas permeability. Then, we define local flux F, which is the product of A_n and Γ_n, as a measure of the local mobility. The local flux F is plotted against P_{O_2} in Figure 7. A positive correlation between F and P_{O_2} is, of course, mainly governed by the relaxation rate Γ_n of the narrow component. It should be noted here that the local flux F varies in a range of 2 orders of magnitude among these polymers, while the gas permeability P_{O_2} does in a range of 4 orders of magnitude as indicated by a straight dashed line in Figure 7. This implies that P_{O_2} is not determined only by the local mobility but also by some other factors such as microvoids, chemical affinity,

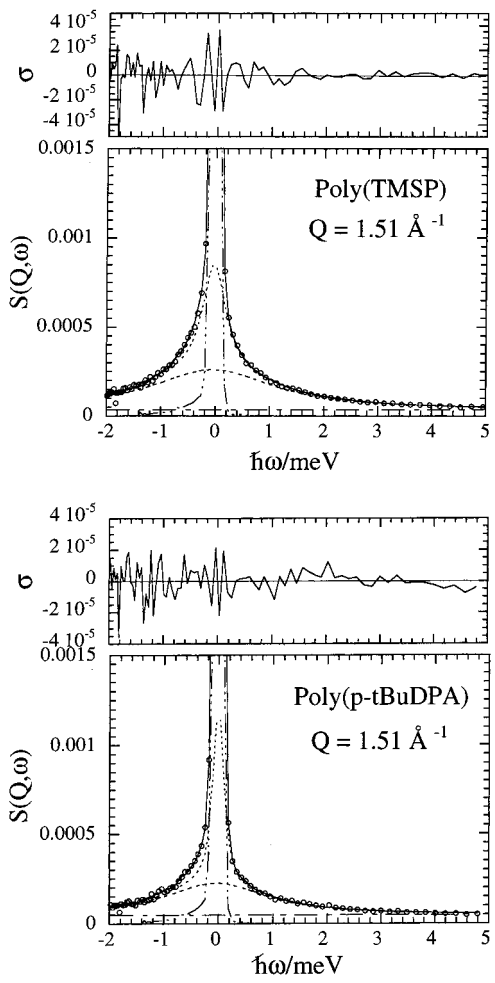

Figure 4. Results of curve fitting using a model function (eq 4) for sample 1 [poly(TMSP)] (a, top) and sample 5 [poly(p-tBuDPA)] (b, bottom): (— - —) inelastic flat background, (- - -) broad component, (- - -) narrow component, (— -- —) elastic component.

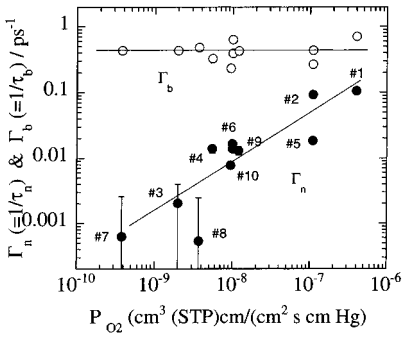

Figure 5. Relaxation rates Γ_n ($=1/\tau_n$) and Γ_b ($=1/\tau_b$) for the narrow and broad components as a function of P_{O_2}.

molecular structure, and so on. It is well-known that the permeability coefficient P_{O_2} is the product of the solubility coefficient S_{O_2} and the diffusion coefficient D_{O_2} in rubbery polymers.

$$P_{O_2} = S_{O_2} D_{O_2} \tag{6}$$

Though eq 6 is an approximation in glassy polymers, we tentatively apply this equation to discuss the relationship with the local flux F in more detail. It is very natural to consider that the local mobility is related not to the solubility coefficient but directly to the diffusion

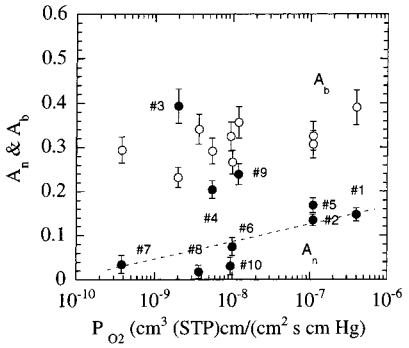

Figure 6. Fractions A_n and A_b of the narrow and broad components as a function of P_{O_2}.

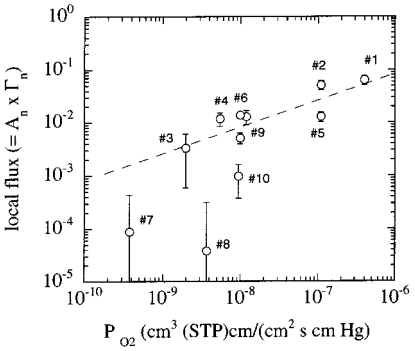

Figure 7. Local flux F ($= \Gamma_n A_n = A_n/\tau_n$) vs P_{O_2} in double-logarithmic form.

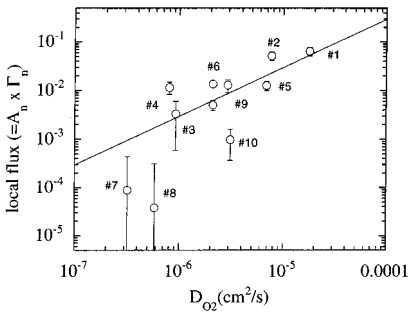

Figure 8. Local flux F ($= \Gamma_n A_n = A_n/\tau_n$) vs D_{O_2} in double-logarithmic form. Slope of the straight line is 1.0.

coefficient. The former must be dominated by chemical affinity and microvoids. In this work, therefore, we have separately estimated S_{O_2} and D_{O_2} (Table 1) and discuss the relationship between the local mobility and the diffusion coefficient.

The local flux F is plotted against the diffusion coefficient D_{O_2} in the double-logarithmic form in Figure 8. The local flux F increases with increasing diffusion coefficient D_{O_2}, and the slope of the log—log plot is unity. This means that the diffusion coefficient is linearly proportional to the local flux, although the scattered data points suggest that the diffusion coefficient is also affected by some other factors such as free volume in polymers.[29] The present result strongly implies that the local mobility is related to the gas permeability through the diffusion coefficient. In the following, we will consider a scenario to explain the present result.

In the glassy state, though the main chain motions are frozen, the local side chain motions are partially active, which are observed as quasielastic scattering in the present measurements. What we found is that the local side chain motion in a time scale of several tens of picoseconds is correlated to the diffusion coefficient; the

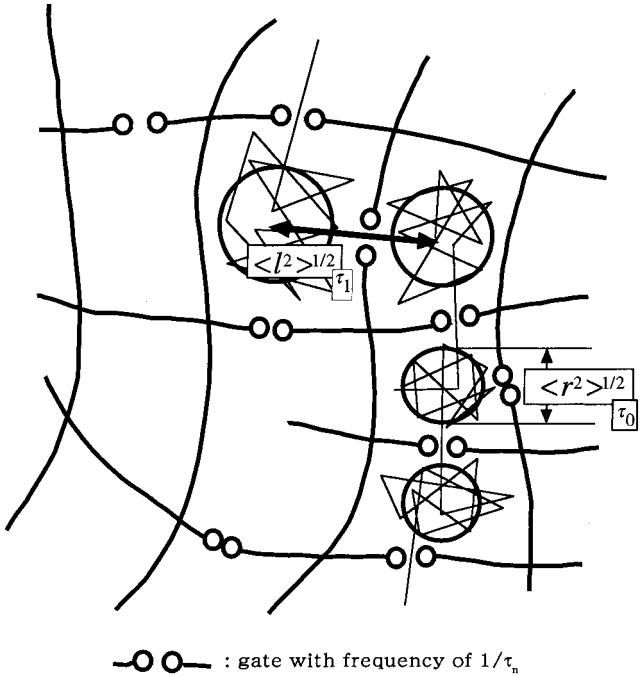

Figure 9. Schematic drawing of the random gate model for substitute polyacetylenes. Note that the solid curves in the figure do not represent polymer chains, but regions that gas molecules cannot go through. τ_0 and τ_1 are the resident time in a cavity and the traveling time from a cavity to another, and $\langle r^2\rangle^{1/2}$ and $\langle l^2\rangle^{1/2}$ are the mean-square displacements in the cavity and the traveling motion from a cavity, respectively.

local flux F is approximately proportional to the diffusion coefficient D_{O_2} ($F \propto D_{O_2}$). To explain this relation, we propose a random gate model as shown in Figure 9. In this model, a gas molecule exists in a cavity in polymer matrix and performs random motions to pass out from a cavity to another through a gate consisting of the mobile side groups. The resident time in the cavity and the traveling time from a cavity to another are denoted as τ_0 and τ_1, respectively. To calculate the macroscopic diffusion coefficient of a gas molecule in this model, we need the mean-square displacements for the random motion in a cavity and the escape motion from a cavity, which are termed $\langle r^2\rangle$ and $\langle l^2\rangle$, respectively. Then, the macroscopic diffusion coefficient is given by[30]

$$D = \frac{\frac{1}{6}(\langle l^2\rangle + 6\langle r^2\rangle)}{\tau_0 + \tau_1} \tag{7}$$

This equation implies that the diffusion coefficient is dominated by both the intracavity motion and the jump motion as a function of the resident time and the traveling time, respectively. How can we estimate these times? First we assume that a gas molecule can escape from a cavity when the gate is open with a frequency of $1/\tau_n$, which is on the order of $\sim$0.01 ps^{-1} (see Figure 5), and the resident time is determined by this frequency, i.e., $\tau_0 \approx \tau_n$ ($\approx$100 ps). The traveling time is roughly evaluated through the relation $\tau_1 = \langle l^2\rangle^{1/2}/v_{O_2}$, where v_{O_2} is the mean velocity of an O_2 gas molecule. This velocity v_{O_2} was calculated from the Maxwell distribution to be 444 m/s (= 4.44 Å/ps) at 298 K, assuming that the velocity of O_2 during the travel from a cavity to another is almost the same as that in the gas state. Putting $\langle l^2\rangle^{1/2}$ = 10 Å, τ_1 is calculated to be $\sim$2 ps. As will be seen later, this is slightly overestimated, and so τ_1 is less than $\sim$2 ps. Then, we obtain a relation $\tau_0 \gg \tau_1$, which means that a gas molecule stays in a cavity for most of its time. In this case, the diffusion coefficient is reduced to[31]

$$D = \frac{\langle l^2\rangle}{6\tau_n} \tag{8}$$

In the above discussion, the fraction of the mobile side groups, which work as gates, was not taken into account. The apparent resident time in a cavity must decrease with increasing the mobile fraction. If we assume a relation between the resident time τ_0 and the mobile fraction A_n, $\tau_0 = \alpha\tau_n/A_n$ (α being a proportional constant), we finally obtain a relation

$$D = \frac{\alpha A_n\langle l^2\rangle}{6\tau_n} = \frac{\alpha\langle l^2\rangle}{6}F \tag{9}$$

This agrees with the observed relation ($F \propto D_{O_2}$), suggesting that the random gate model is a candidate that can explain the role of local mobility in the gas permeability of substituted polyacetylenes. The resident time is also dominated by other factors such as the size of the gate, but these were not taken into account in this model for simplicity.

Using eq 9 and assuming $\alpha A_n = 1$, the mean-square displacement $\langle l^2\rangle^{1/2}$ of the O_2 molecule was calculated from the observed D_{O_2} and τ_n and is listed in Table 1. The values of $\langle l^2\rangle^{1/2}$ are in the range of $\sim$2 to $\sim$8 Å, corresponding to 0.66 to 2.7 times as large as the diameter of an oxygen molecule (3 Å). This implies that the oxygen gas does not perform large distance jumps, but small jumps in the substituted polyacetylenes.

Finally, we would like to discuss the modes of the motions in the substituted polyacetylenes. In the past two decades, extensive studies have been performed regarding the dynamics of glassy polymers from a microscopic point of view.[32,33] It is now well-known that there is an excitation characteristic of glasses far below the glass transition temperature T_g, the so-called Boson peak, observed in an energy range of 2−4 meV, irrespective of chemical structure. With increasing temperature, the intensity of the Boson peak increases according to the Bose−Einstein population factor. As temperature further increases, anharmonic excess quasielastic scattering, the so-called fast process, appears in an energy range below the Boson peak or in a time region of picoseconds. The onset temperature depends on the kind of polymers; it is $\sim$50 K below T_g in the polymers with no or small side groups such as polybutadiene[21,34] and polychloroprene,[23] while it appears far below T_g in polymers with either relatively large side groups or internal degrees of freedom.[22,35,36] In the substituted polyacetylenes studied here, the Boson peak is not observed at 298 K and the dynamic scattering law looks quasielastic-like, suggesting that the fast process appears at 298 K or below. The present analysis indicates that the dynamic scattering laws $S(Q,\omega)$ of the substituted polyacetylenes are described by the sum of a δ-function, two Lorentzians, and the inelastic flat background. By analogy with other glassy polymers,[22,23] the broad Lorentzian and the inelastic flat background can be assigned to the fast process and the overdamped Boson peak, respectively. Relaxation motions similar to the narrow component with the relaxation time of several tens of picoseconds have never been observed so far below T_g in simple polymers such as

polybutadiene, polyisobutylene, polychloroprene, and polyethylene,[37] but only above T_g. In these polymers, the motions have been assigned to the main chain motions accompanied by conformational transitions. In the substituted polyacetylenes, however, there are many large side groups which can move even below T_g, and relaxation motions in the time range of several tens of picoseconds may arise from the large side groups and assist the diffusion of gases. In other words, such slow motions are essential for high gas permeability, more specifically for high gas diffusivity, in glassy polymer films.

Conclusion

In this study, we have investigated local motions of 10 substituted polyacetylenes using a quasielastic neutron scattering technique in a time range of picoseconds to several tens of picoseconds. The observed quasielastic scattering component in the dynamic scattering law $S(Q,\omega)$ was successfully described by the sum of two Lorentzians: the narrow (slow) and broad (fast) components. It was found that the relaxation rate Γ_n (inverse of the relaxation time τ_n^{-1}) and the fractions A_n of the narrow (slow) component show a positive correlation with the oxygen permeability coefficient, P_{O_2}, especially with the diffusion coefficient of O_2, D_{O_2}, while those of the broad (fast) component do not, suggesting that the narrow component plays an important role in the gas permeability of the substituted polyacetylenes. We then defined local flux F, which is the product of the relaxation rate Γ_n and the fraction A_n ($F = \Gamma_n A_n$), as a measure of the local mobility and found that F is approximately proportional to the diffusion coefficient $F \propto D_{O_2}$. To explain how the local mobility of the matrix polymer is associated with the gas diffusion, we have proposed the random gate model, in which gas molecules diffuse through the gates consisting of mobile side groups. Qualitatively, this model predicts the relation of $F \propto D_{O_2}$.

Thus, this study has demonstrated that the local mobility plays an important role in the gas permeability at least in a series of substituted polyacetylens. It should be noted that the gas permeability is determined by many factors such as microvoid, chemical affinity between gas and matrix polymers, molecular structure, and local mobility and further that the significance of local mobility should depend on the kind of polymer. It is therefore a challenging work to clarify roles of local mobility in other polymer systems such as flexible vinyl polymers.

Acknowledgment. We are grateful to Prof. T. Kajitani and Dr. S. Shamoto for the support of neutron scattering measurements and to Prof. Y. Tsujita for valuable discussions.

References and Notes

(1) *Polymer Membranes for Gas and Vapor Separation: Chemistry and Materials Science*; Freeman, B. D., Pinnau, I., Eds.; American Chemical Society: Washington, DC, 1999.
(2) Kesting, R. E.; Fritzsche, A. K. *Polymeric Gas Separation Membrances*; Wiley: New York, 1993.
(3) Nagai, K.; Masuda, T.; Nakagawa, T.; Freeman, B. D.; Pinnau, I. *Prog. Polym. Sci.* **2001**, *26*, 721−798.
(4) Masuda, T.; Isobe, E.; Higashimura, T.; Takada, K. *J. Am. Chem. Soc.* **1983**, *105*, 7473−7474.
(5) Ichiraku, Y.; Stern, S. A.; Nakagawa, T. *J. Membr. Sci.* **1987**, *34*, 5−18.
(6) Masuda, T.; Iguchi, Y.; Tang, B.-Z.; Higashimura, T. *Polymer* **1988**, *29*, 2041−2049.
(7) Witchey-Lakshmanan, L. C.; Hopfenberg, H. B.; Chern, R. T. *J. Membr. Sci.* **1990**, *48*, 321−331.
(8) Robeson, L. M.; Burgoyne, W. F.; Langsam, M.; Savoca, A. C.; Tien, C. F. *Polymer* **1994**, *35*, 4970−4978.
(9) Isobe, E.; Masuda, T.; Higashimura, T.; Yamamoto, A. *J. Polym. Sci., Polym. Chem. Ed.* **1986**, *24*, 1839−1848.
(10) Masuda, T.; Isobe, E.; Hamano, T.; Higashimura, T. *J. Polym. Sci., Polym. Chem. Ed.* **1987**, *25*, 1353−1362.
(11) Tsuchihara, K.; Masuda, T.; Higashimura, T. *J. Am. Chem. Soc.* **1991**, *113*, 8548−8549.
(12) Tsuchihara, K.; Masuda, T.; Higashimura, T. *Macromolecules* **1992**, *25*, 5816−5820.
(13) Toy, L. G.; Nagai, K.; Freeman, B. D.; Pinnau, I.; He, Z.; Masuda, T.; Teraguchi, M.; Yampolskii, Y. P. *Macromolecules* **2000**, *33*, 2516−2524.
(14) Kouzai, H.; Masuda, T.; Higashimura, T. **1994**, *32*, 2523−2530.
(15) Ito, H.; Masuda, T.; Higashimura, T. *J. Polym. Sci., Part A: Polym. Chem.* **1996**, *34*, 2925−2925.
(16) Teraguchi, M.; Masuda, T. *J. Polym. Sci., Part A: Polym. Chem.* **1998**, *36*, 2721−2725.
(17) Nagai, K.; Toy, L. G.; Freeman, B. D.; Teraguchi, M.; Masuda, T.; Pinnau, I. *J. Polym. Sci., Part B: Polym. Phys.* **2000**, *38*, 1474−1484.
(18) Bee, M. *Quasielastic Neutron Scattering. Principles and Applications in Solid State Chemistry, Biology and Materials Science*; Adam Hilger: Bristol, 1988.
(19) Kanaya, T.; Kaji, K.; Ikeda, S.; Inoue, K. *Chem. Phys. Lett.* **1988**, *150*, 334−338.
(20) Inoue, K.; Kanaya, T.; Ikeda, S.; Kaji, K.; Shibata, K.; Misawa, M.; Kiyanagi, Y. *J. Chem. Phys.* **1991**, *95*, 5332−5340.
(21) Kanaya, T.; Kawaguchi, T.; Kaji, K. *J. Chem. Phys.* **1993**, *98*, 8262−8270.
(22) Kanaya, T.; Kawaguchi, T.; Kaji, K. *J. Chem. Phys.* **1996**, *104*, 3841−3850.
(23) Kanaya, T.; Kawaguchi, T.; Kaji, K. *J. Chem. Phys.* **1996**, *105*, 4342−4349.
(24) Kanaya, T.; Teraguchi, M.; Masuda, T.; Kaji, K. *Polymer* **1999**, *40*, 7157−7161.
(25) Kanaya, T.; Tsukushi, I.; Kaji, K.; Teraguchi, M.; Kwak, G.; Masuda, T. *J. Phys. Soc., Suppl. A* **2000**, *70*, 332−334.
(26) Masuda, T.; Okano, Y.; Kuwane, Y.; Higashimura, T. *Polym. J.* **1980**, *12*, 907−913.
(27) Kajitani, T.; Shibata, K.; Ikeda, S.; Kohgi, M.; Yoshizawa, H.; Nemoto, K.; Suzuki, K. *Physica* **1995**, *213/214*, 872−874.
(28) Bacon, G. E. *Neutron Diffraction*; Clarendon Press: Oxford, 1975.
(29) Ito, K.; Saito, Y.; Yamamoto, T.; Ujihira, Y.; Nomura, K. *Macromolecules* **2001**, *34*, 6153−6155.
(30) Singwi, K. S.; Sjolander, A. *Phys. Rev.* **1960**, *119*, 863−871.
(31) Springer, T. *Quasielastic Neutron Scattering for the Investigation of Diffusive Motions in Solids and Liquids*; Springer-Verlag: Berlin, 1972.
(32) *Yukawa International Seminar 1996 (YKIS'96), Prog. Theor. Phys. Suppl.* **1997**, *126;* Odagaki, T., Hiwatari, Y., Matsui, J., Eds.; Yukawa Institute for Theoretical Physics: Kyoto, 1997.
(33) *The Third International Discussion Meeting on Relaxation in Complex Systems; J. Non-Cryst. Solids* **1998,** *235/237* ; Ngai, K. L., Riande, E., Ingram, M. D., Eds.; Elsevier: Amsterdam, 1997.
(34) Frick, B.; Richter, D.; Petry, W.; Buchenau, U. *Z. Phys. B: Condens. Matter* **1988**, *70*, 73−79.
(35) Buchenau, U.; Schönfeld, C.; Richter, D.; Kanaya, T.; Kaji, K.; Wehrmann, R. *Phys. Rev. Lett.* **1994**, *73*, 2344−2347.
(36) Hansen, J.; Kanaya, T.; Nishida, K.; Kaji, K.; Tanaka, K.; Yamaguchi, A. *J. Chem. Phys.* **1998**, *108*, 6492−6497.
(37) Kanaya, T.; Kawaguchi, T.; Kaji, K. *Macromolecules* **1999**, *32*, 1672−1678.

MA0203546